Sensors and Actuators A 232 (2015) 285–291

Contents lists available at ScienceDirect

Sensors and Actuators A: Physical

journal homepage: www.elsevier.com/locate/sna

Flexible phototransistors based on graphene nanoribbon decorated with MoS_2 nanoparticles

Mohsen Asad[a,*], Sedigheh Salimian[b], Mohammad Hossein Sheikhi[a], Mahdi Pourfath[c,d]

[a] School of Electrical and Computer Engineering, Shiraz University, Shiraz 71345-1585, Iran
[b] Faculty of Physics, Kharazmi University, Tehran 15719-14911, Iran
[c] School of Electrical and Computer Engineering, University of Tehran, Tehran 14395-515, Iran
[d] Institute for Microelectronics, TU Wien, Gußhausstraße 27–29/E360, A-1040 Wien, Austria

ARTICLE INFO

Article history:
Received 28 February 2015
Received in revised form 16 June 2015
Accepted 17 June 2015
Available online 22 June 2015

Keywords:
Graphene nanoribbon
MoS_2 nanoparticles
Photo-transistor
Photo-responsivity
Photo-switching

ABSTRACT

This paper presents highly efficient, flexible, and low-cost photo-transistors based on graphene nanoribbon (GNR) decorated with MoS_2 nanoparticles (NPs). Due to high carrier mobility, GNR has been used as carrier transport channel and MoS_2 NPs provide strong advantage of high gain absorption and the generation of electron-hole pairs. These pairs get separated at the interface between GNR and MoS_2 NPs, which leads to electron transfer from NPs towards GNR. The fabricated devices based on GNR-MoS_2 hybrid material show a high photo-responsivity of 66 A W^{-1} and fast rise-time (t_r) and decay-time (t_d) of 5 ms and 30 ms, respectively, under blue laser illumination with a wavelength of 385 nm and power density of 2.1 μW. The achieved photo-responsivity is 1.3×10^5 and 10^4 times larger than that of the first reported pristine graphene and MoS_2 photo-transistors, respectively. Furthermore, fabricated devices show a high stability for bending radii larger than 6 mm. The simple solution based process, high gain and reproducible operation of fabricated photo-transistors indicate potential applications of them in state of the art photo-detectors and imaging systems.

1. Introduction

In recent years, two-dimensional materials provide an emerging class of potential practical applications, due to their unique electrical and mechanical properties. Graphene or single layered graphite has introduced great era for fabrication of nanoscale devices because of its crystal structure and semimetal electrical properties [1–3]. Because of linear relation between energy and momentum, two-dimensional structure of graphene behaves as massless Dirac fermion [1,4,5]. Furthermore, carriers in graphene describe by relativistic Dirac equation, which exhibit zero mass and effective speed of 10^6 m s^{-1} (near speed of light). At the same time, zero energy bandgap between the highest occupied molecular orbital (HOMO) and lowest unoccupied molecular orbital (LUMO) provides ballistic transport for charge carrier for potential application in ultrafast electronic devices [6,7]. In addition, to induce an electric band gap, a graphene sheet can be tailored into nanoribbon, where the energy gap is inversely proportional to the ribbon's width [8–11]. This unique properties of band structure in graphene delivers wavelength independent opacity [12] and thermal conductivity [13], suitable for optoelectronic applications.

Because of spectral band width and ultrafast response time, graphene has been introduced as a promising material for photo-detectors [14–18]. However, due to low light absorption in graphene photo-responsivity (the generated current per incident optical power) less than 10^{-2} A W^{-1} has been obtained [14–18]. One of the main reasons for low photo-responsivity of graphene is fast recombination of photogenerated carriers before reaching to electrodes or any p–n junction, which are necessary for electron–hole separation in photo-detectors. Different strategies such as thermoelectric effect [19–21] or graphene plasmonics [22] have been used to improve light absorption in graphene. Implementation of photoconductive gain – the ability to provide multiple carrier per single incident photon – is one of the recommended solution for ultrafast graphene photo-detectors to make them more practical.

Large surface area with high density of states, make graphene an attractive choice as matrices for interfacing with inorganic nanostructures [23]. Due to atomically thickness of graphene, its conductance is very sensitive to any electrostatic perturbation by chemical or physical experience close to the surface.

* Corresponding author. Fax: +98 711 614218.
E-mail address: mohsenasad@shirazu.ac.ir (M. Asad).

http://dx.doi.org/10.1016/j.sna.2015.06.018
0924-4247/

Considering this advantage, functionalization of graphene with other nanostructure can emerge a new class of application combining advantage of nanostructures [24] and graphene [25]. Photo-detectors based on graphene matrices decorated with nanoparticles have been previously demonstrated [26,27].

On the other hand, molybdenum disulfide (MoS_2) — a transition metal dichalcogenide (TMD) with a direct bandgap (~1.8 eV for monolayer and ~1.3 eV for bulk) — has received much interest for nanoscale electronics on various type of substrate [28–34]. Due to large surface to volume ratio, high carrier mobility (~700 cm^2/V-s at room temperature) [35] and high mechanical strength [36], MoS_2 is a compelling semiconductor for sensor application and flexible electronics. High gain photo-transistor with photo-responsivity from 7.5 mA W^{-1} to 880 A W^{-1} and fast optical switching have been reported by different groups [38–41].

Synthesis of heterostructure of graphene and single layer MoS_2 have attracted interest because of two dimensionality of both materials [42–44]. Combining excellent properties of MoS_2 NPs and GNR, a low cost, flexible, efficient photo-detector is demonstrated in this work, where the MoS_2 NPs are used as photon absorber. The photo-excited electron–hole pairs at the surface of the nanoparticles act as photo-induced gate which perturb the carrier transport in the GNR channel through electrostatic coupling. The photo-transistors based on the GNR-MoS_2 NPs heterostructures show photo-responsivity value higher than 66 A W^{-1}.

2. Experimental

2.1. GNR-MoS_2 NPs heterostructures preparation

Here, we describe a simple solution based process to decorate GNR with MoS_2 NPs. Oxidized graphene nano ribbon (GO) was obtained according to unzipping of MWCNT by the method reported by Kosynkin et al. [45]. 100 mg of MWCNTs was suspended in sulphuric acid for 2 h, followed by treatment with 600 wt% $KMnO_4$ for 2 h at room temperature. Then the solution was stirred about 1 h. Oxidized graphene nanoribbon was obtained after several washing of the solution with HCl and ethanol and filtration by PTFE membrane (with 0.45 μm pore).

Then, 15 mg GO was dispersed in 20 ml of DMF and the solution was stirred 30 min. In photo-detector applications, for tuning the cut-off wavelength, the size of NPs is controlled by varying the process parameters such as; solvent to surfactant molar ratio, reagent concentration and process time. Here, in order to adjust the adsorption wavelength, various concentrations of GNR/$(NH_4)_2MoS_4$ from 1.5 to 3 with 4 steps have been used with respect to constant DMF volume. Afterward, 10 mg, 8 mg, 7 mg and 5 mg-ratio from 1.5 to 3, respectively- of $(NH_4)_2MoS_4$ were added to the separate solutions and each suspension was stirred 30 min at room temperature until a clear brown solution was obtained. After that, 2 mg hydrazine was added to solution and stirring was continued for 45 min to reduce the graphene oxides to graphene nanoribbon. Then, solution was transferred to a 60 ml Teflon-lined autoclave and was heated at 210 °C for 10 h in a standard oven without any controlled temperature ramp. Centrifugation process at 6000 rpm for 15 min was used to collect the final nano hybrid material. Annealing of powder was carried out in presence of H_2 at 60 °C for 1 h to saturate any dangling bonds and reduce scattering sites alongside GNR.

2.2. Device fabrication

Compared with the rigid and flat substrates like silicon wafers and glass plates, polymers are light, flexible, cheap and easy to adjust their material properties. Especially, polyethylene tetraphtalate (PET) film was widely used as a substrate for various kind of devices due to its transparency, flexibility, thermal resistance and mechanical strength [46,47]. The flexible devices were fabricated on PET substrates with a thickness of 150 μm. Photoresist can be spin-coated on the PET by direct dispensing technique using micropipette. Since the PET film has flexible and relatively rough surface, the thickness of photoresist layer may not be uniform. This non-uniform coating of resist normally produced non-uniform lift-off process and some patterns may be disrupted. In order to prevent the formation of non-uniformity, thin layer of resist was used. The resist was spin coated on PET substrate at 3000 rpm for 30 s. After spin coating, PET film was baked at 90 °C for 2 min. Source and drain were patterned using conventional lithography for 100 μm channel length. Then the 20 nm thick Cr film was deposited as adhesive layer, and 200 nm Al was deposited on it using sputtering system (Yar Nikan Saleh Co., Iran). Deposition was followed by lift-off and interdigit (IDT) patterns were fabricated successfully. Then 200 nm Al was also coated on backside of the PET, resulting in a back-gate structure.

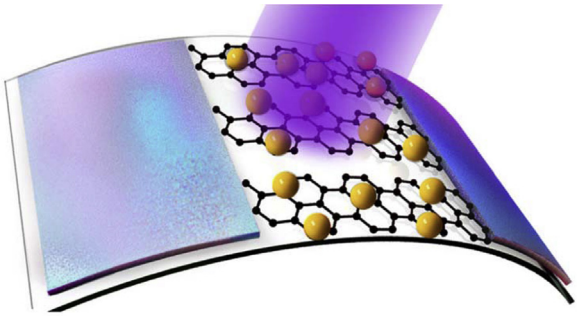

Fig. 1. The schematic structure of the fabricated photo-transistor based on GNR-MoS_2 NPs.

10 mg of nanomaterial with GNR/$(NH_4)_2MoS_4$ ratio of 1.5 were dispersed in 20 ml DMF, then sonicated for 10 min to obtain a homogenous solution. The suspension was then spin coated on Al electrodes at 600 rpm and GNR-MoS_2 NPs have randomly arranged between source and drain. Finally, the samples were annealed at 60 °C for 5 min. The schematic of the fabricated device is shown in Fig. 1.

2.3. Characterization

Raman spectra was recorded at ambient temperature using a standard backscattering geometry. Excitation wavelength of 785 nm were produced by a high-power laser diode source capable of supplying 50 mW of power. Optical spectroscopy at UV–vis region was employed to investigate the optical absorption and cut-off wavelength. Morphology of the nanostructures were studied using transmission electron microscopy (TEM, model Philips EM208) operated at 100 kV. Elemental composition of the final nanomaterial was analyzed by energy dispersive spectroscopy (EDS) using Zeiss scanning electron microscopy (SEM) equipped with Oxford Instruments. Photo-response of the fabricated photo-transistors were investigated with standard optoelectronic set-up consist of focused beam blue laser (λ = 385 nm) and at various illumination intensities by measuring drain-source current (I_{DS}) versus change of drain-source voltage (V_{DS}) and backgate voltage (V_{BG}). The devices were characterized before and after the bending tests. In the bending tests, the flexible samples were bent up to a radius of 7 mm and the conductance was measured in each point.

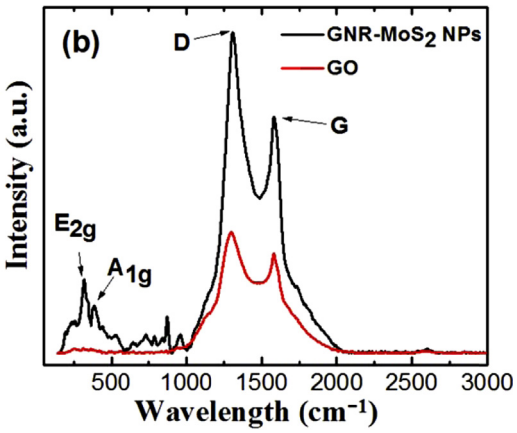

Fig. 2. Raman spectra of graphene oxide (red) and GNR-MoS_2 NPs (black).

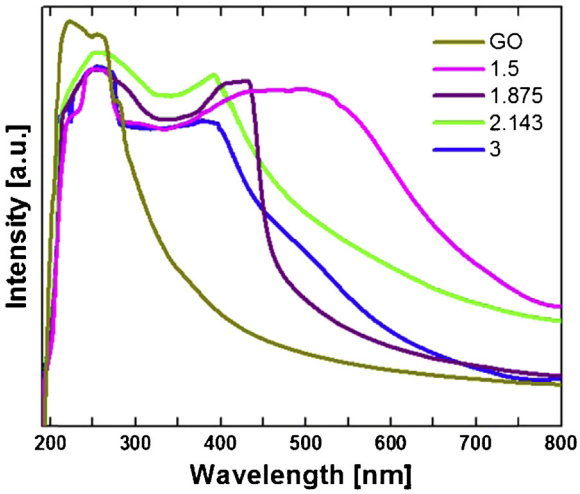

Fig. 3. UV–vis spectrum of the GO and GNR after decoration with MoS_2 NPs at 210 °C for 10 h with various ratio of GNR/$(NH_4)_2MoS_4$ of 1.5, 1.875, 2.143 and 3.

3. Results and discussions

3.1. Raman spectroscopy

The Raman spectra of GNR-MoS_2 NPs nanomaterial is shown in Fig. 2 and compared to the corresponding spectra for the graphene oxide nanoribbon. Several locations on each sample surface were probed in Raman spectroscopy to ensure reproducibility of the data. G band and D band of appearing at 1596 cm^{-1} and 1359 cm^{-1} are originated from the Raman active mode of the graphene. The displacement in the G band to 1540 cm^{-1} is and evidence of removing of the oxygnerated functional group after reduction process. In addition, a comparison of intensity ratio of I(D)/I(G) peaks is utilized to characterize the reduction of graphene oxide [48], whereas, the increase in this ratio is attributed to new graphitic domain generated during reduction of GO [49]. This relatively low intensity of I(D)/I(G) suggests the presence of nanoscopic hole in the graphene plane or small size of the sp^2 domains [50]. Furthermore, Fig. 2 shows two Raman active modes of E_{2g} and A_{1g} at 377 cm^{-1} and 403 cm^{-1} which are associated with the vibrational phonons of MoS_2 NPs [51]. By decreasing the MoS_2 particle size, a large density of state can be produced by zone-edge phonons [52] which cause additional disorder peaks. Using the 785 nm laser energy excitation can also cause extreme features in the phonon density of states near the phonon energies which leads to disorder peaks near 750 cm^{-1} [53].

3.2. UV–vis spectroscopy

Fig. 3 shows the cut-off wavelengths of 680 nm, 505 nm, 500 nm and 500 nm for the various ratio of GNR/$(NH_4)_2MoS_4$ of 1.5, 1.875, 2.143 and 3, respectively. The measurement reveals the cut-off wavelength of 680 nm and 500 nm in final hybrid nanomaterials consistent with few-layer and mono-layer of MoS_2 [36,37] and disclose the spectral selectivity of the nano-heterostructures (NHs) because of the bandgap tenability of NPs by controlling the parameters of process [27]. As shown in the UV–vis spectrum (Fig. 3), the absorption peak of GO (230 nm) corresponding to a π–π^* absorption band of aromatic C=C bonds and an n–π^* absorption band at 295 nm are appeared [54]. The redshift of π–π^* to 265 nm for GO after decoration with MoS_2 NPs, may suggest the reduction of graphene oxide [55]. The increased absorption intensity of the entire spectrum above the 300 nm region, offered the reduction of the GO and restoration of the aromatic structure gradually [56].

3.3. Morphological study and EDS analysis

TEM was used to investigate the morphology of NHs. Fig. 4a shows that sidewalls of MWCNT being completely unzipped with smooth edges. The successive opening reaction can be attributed to amount (500 wt%) of oxidation agent ($KmNO_4$) introduced to system for unzipping. Fig. 4b presents the MoS_2 NPs after thermal decomposition of $(NH_4)_2MoS_4$ with a diameter of about 100 nm. The decomposition process leads to MoS_3 and ammonia and hydrogen sulfide, starting at 155 °C [57]. Then MoS_2 NPs obtain by decomposition of MoS_3 in temperature range of 300–820 °C by various crystal quality [58]. The decomposition processes are mentioned below:

$$(NH4)_2MoS_4 \rightarrow MoS_3 + 2NH_3 + H_2S \text{at} 155\,^{\circ}C \quad (1)$$

$$MoS_3 \rightarrow MoS_2 + S \text{at} 800\,^{\circ}C \quad (2)$$

Fig. 4c confirms the attachment of MoS_2 NPs on the graphene nanoribbon, suggesting successful association of MoS_2 NPs with the reduced graphene nanoribbon. Fig 4c (right TEM image) also reveals the effective coverage of GNR with MoS_2 NPs. The EDS analysis is presented in Fig. 4d while, the y axis presents the number of counts per element. Carbon, Mo and S elements indexed in the EDS spectra indicate the presence of the graphene and MoS_2 NPs in the final product.

3.4. Photo-response characterization

For assessing the ohmic properties of the fabricated devices, electrical characterization was performed under different illumination intensity of 0.18 μW, 0.58 μW and 2.1 μW with a focused beam blue laser (λ = 385 nm). Maximum illumination intensity of 0.1 W cm^{-2} for a 50 μm diameter spot size has been obtained using a stage controlled objective lens. Fig. 5a presents the I_{DS}–V_{DS} characteristics of the photo-transistors under different illumination intensities and V_{BG} = 0 V. The decreased I_{DS} for higher power density demonstrates effective relation between carrier-charge density and electron–hole pair generation in the GNR-MoS_2 NPs hybrid material. Linear dependence of the photo-current on the V_{DS} also presents the ohmic contact behavior of the devices. At low illumination power of 0.21 μW, the device reaches the photo-responsivity of 66 A W^{-1}, ~1.3×10^5 times higher than the first graphene photodetectors [17] and ~10^4 time higher than first single layer MoS_2 photo-transistors [38]. Zhang et al., recently introduced a

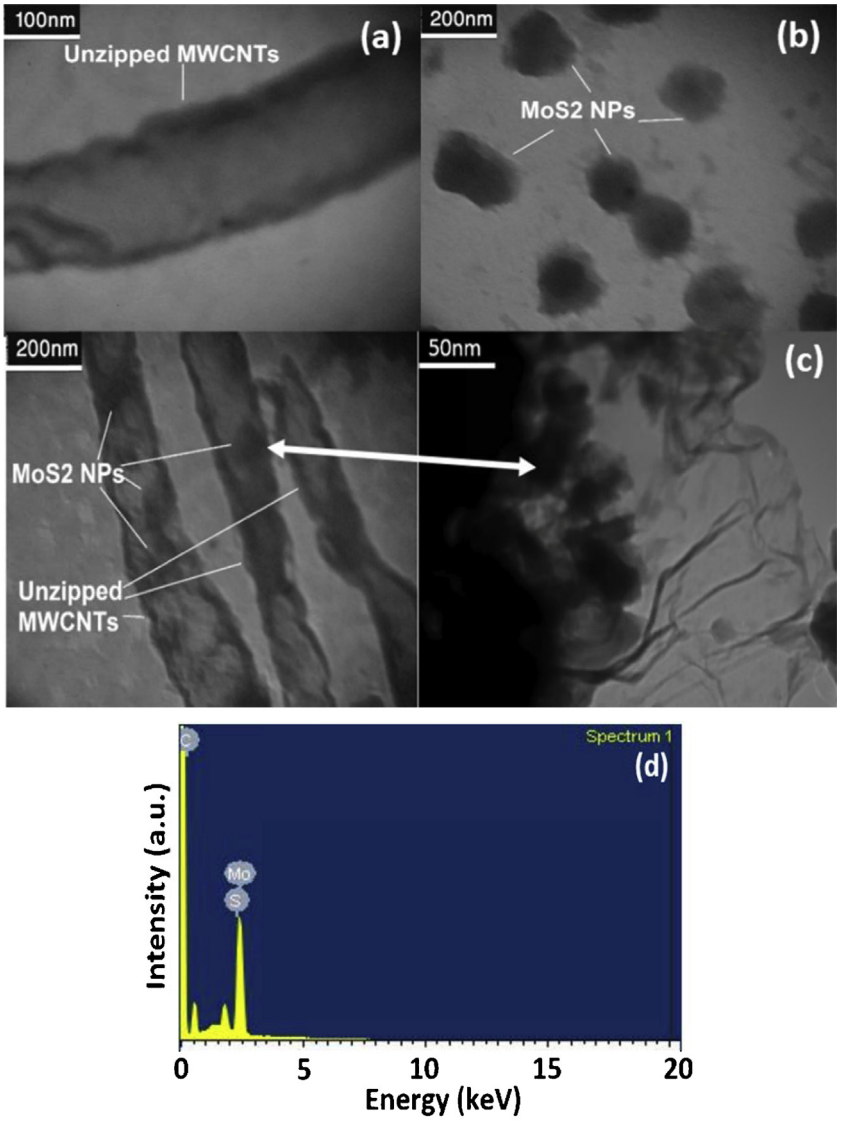

Fig. 4. TEM images of (a) reduced unzipped MWCNT obtained after treatment with N_2H_4 (b) MoS_2 NPs obtained by thermal decomposition of $(NH_4)_2MoS_4$ (c) GNR decorated with MoS_2 NPs, (right image shows GNR is covered with MoS_2), (d) EDS analysis of GNR-MoS_2 NPs nano heterostructure which reveals presence of Mo, S and C.

photo-transistor based on graphene-MoS_2 heterostructure with photo-responsivity of 10^7 A W^{-1} [58]. This high photo-responsivity can be attributed to large area and continues CVD grown monolayer MoS_2 with effective transferring of graphene on it with minimum defects. Li et al., also reported a self-powered graphene-MoS_2 hybrid photo-transistor with photo-responsivity of 3 AW^{-1} [59]. This low photo-responsivity arises from low photo-carrier injection from mechanically exfoliated few-layer MoS_2 towards graphene because of high defect density in scotch-tape based mechanical exfoliation of bulk MoS_2. Fig. 5b shows the dependence of the conductance on backgate voltage at different power densities. In the dark condition, photo-transistor shows the charge neutral point (V_{CNP}) at about V_{BG} = 10 V. The positive V_{CNP} indicates that holes – like pristine p-dope graphene- are dominated carriers in the photo-transistor channel. This feature can be attributed to more conductivity property of the graphene compare to MoS_2. The blue laser illumination upon photo-transistors shifts the V_{CNP} towards more negative voltage. This negative shift demonstrates the photo-gating effect [27] which photo-generated electron-hole pairs separate at graphene-MoS_2 interface and electrons transferred from MoS_2 NPs to graphene which is consistent with previous result by Zhang et al., [58]. At the same time, increasing the conductance at n-type channel ($V_{BG} > V_{CNP}$) and decreasing the conductance at p-type channel ($V_{BG} < V_{CNP}$) reveal that photogenerated electrons are transferred carriers from MoS_2 NPs to graphene. This can be explained by bandgap alignment at the interface of MoS_2 NPs and GNR, as shown in Fig. 5c. The p-type graphene- due to electrostatic doping- has more unoccupied states contributing to transport between source and drain [60]. By type conversion from p-type to n-type, a large number of unoccupied states are unavailable and fewer states contribute to transport mechanism near Fermi level.

To understand the time dependent photo-response of the photo-transistors, exposed to blue laser (λ = 385 nm), the rise-time (t_r) upon turning on the light and decay-time (t_d) upon turning off the light have been characterized at V_{DS} = 1 V and V_{DS} = 10 V. Fig. 6a shows the photo-response of the fabricate photo-transistor which reveals $t_r \approx 5$ ms and $t_d \approx 30$ ms. In consistent with previous reports [58,59], the fast rise-time of the fabricated photo-detector can be due to fast band-to-band excitation of the photo-excited electron-hole pairs between MoS_2 and GNR because of low defect density in MoS_2 NPs and their interface with graphene, as previously reported for SWCNTs decorated with PbS NPs [46]. The dominant part of

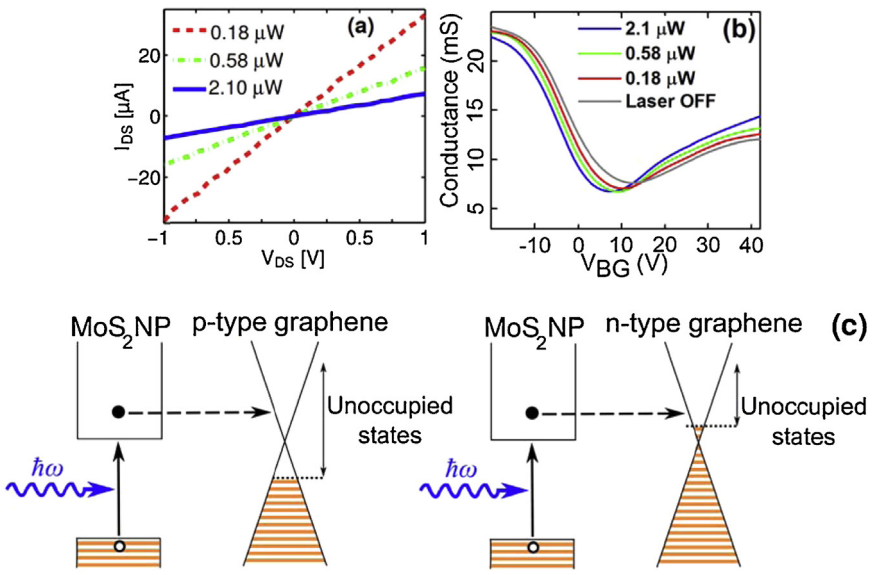

Fig. 5. (a) Drain-source current (I_{DS}–V_{DS}) characteristics under different illumination power densities. (b) Shift of charge natural point voltage under various illumination power densities which reveals photo-gating effect. Shift towards negative voltage demonstrates electron transferring from NPs to graphene. (c) Schematic of the bandgap alignment at MoS_2 NPs and graphene interface for p-type and n-type graphene. Schematic shows the effect of type conversion on the transport prompted states.

decay-time of fabricated photo-transistor is originated from life-time (t_l) of the trapped positive charges in the MoS_2 NPs which produce photo-gating effect that, decay time could be ascribed from the excitation between the defect or charge impurity states and the band edge. As proposed by Konstantatos et al. [27], the decay-time can be reached to smaller values by reducing the potential barrier between trapped charges at NPs and graphene using an electro-static doping. In photo-conductive detectors, photo-current gain can be enhanced by tuning the mobility of the carriers and consequently transit-time (t_{ransit}) which $t_{ransit} = L^2/(\mu V_{bias})$ where, L is source-drain distance and μ is the mobility of the carrier at the active region [61]. In Fig. 6a, enhanced carrier drift velocity due to increased V_{DS} is the main cause of the reduced carrier transit-time (t_{ransit}) which improves the photo-current of the illuminated devices. As shown in Fig. 6a, the fabricated photo-transistor also shows reproducible photo-switching response under repeated on-off cycles of blue laser diode.

In order to evaluate the effect of bending on response of the photo-transistors, the conductance was measured under 2.1 μW illumination power and $V_{BG} = 0$ V as a function of the bending radius. As shown in Fig. 6b, after repeatedly bending in each radius, the photo-response found to be highly stable for bending radii larger than 6 mm. For smaller bending radii, however, the conductance of the photo-transistor is significantly reduced and does not revert back to the original value.

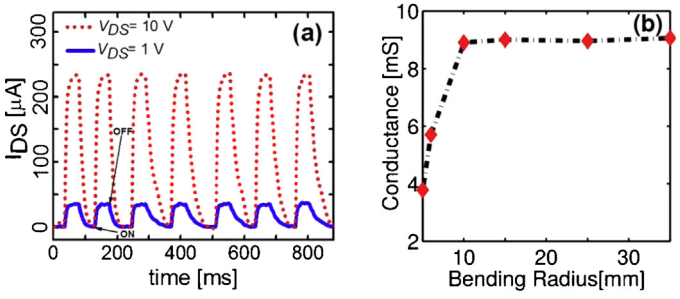

Fig. 6. (a) Time dependent photo-response of the photo-transistor under blue laser (λ = 385 nm) illumination power density of 2.1 μW, $V_{BG} = 0$ V and different drain-source bias voltages of $V_{DS} = 1$ V and $V_{DS} = 10$ V. (b) Effect of bending radius on the conductance of the photo-transistor under illumination intensity of 2.1 μW at $V_{BG} = 0$ V and $V_{DS} = 1$ V.

4. Conclusion

In summary, we have fabricated photo-transistors based on graphene nanoribbons decorated with MoS_2 NPs hybrid material as photo-absorption active area. Graphene nanoribbons act as fast carrier transfer channel and MoS_2 NPs act as photo-harvesting elements at λ = 385 nm in the final devices. Raman and UV–vis spectroscopy has been carried out to investigate the chemical bonds and optical properties of the final materials. Morphology and elemental composition of the GNR-MoS_2 NPs has been evaluated using TEM and EDS analysis to ensure on the final structure of the material. Our photo-transistors showed a photo-responsivity of 66 A W^{-1} which is ~1.3×10^5 times higher than the first demonstrated graphene photo-detectors and ~10^4 time higher than first single layer MoS_2 photo-transistors. Furthermore, the effect of the back-gate voltage on the device operation has been evaluated, which reveals more conductance at negative backgate bias due to more unoccupied states in p-type graphene. Rise-time and decay-time of 5 ms and 30 ms have been obtained, respectively, which demonstrate the low defect density in MoS_2 NPs and their interface with graphene. Photogenerated trapped holes in the NPs induced photo-gating effect, which shifted I_D–V_{BG} characteristics towards more negative voltages. According to low-cost and simple process of NP decoration on graphene nanoribbons, this hybrid material has a high potential to be used in state of the art applications such as low-cost high gain photo-transistors and imaging systems.

References

[1] A.K. Geim, K.S. Novoselov, The rise of graphene, Nat. Mater. 6 (2007) 183–191.
[2] K.S. Novoselov, A.K. Geim, S.V. Morozov, D. Jiang, M.I. Katsnelson, I.V. Grigorieva, S.V. Dubonos, A.A. Firsov, Two-dimensional gas of massless dirac fermions in graphene, Nature 438 (2005) 197–200.
[3] Y. Zhang, Y.W. Tan, H.L. Stormer, P. Kim, Experimental observation of the quantum hall effect and Berry's phase in graphene, Nature 438 (2005) 201–204.

[4] J.C. Charlier, P.C. Eklund, J. Zhu, A.C. Ferrari, Electron and phonon properties of graphene: their relationship with carbon nanotubes, Top. Appl. Phys. 111 (2008) 673–709.
[5] P.R. Wallace, The band theory of graphite, Phys. Rev. 71 (1974) 622–634.
[6] F. Chen, N.J. Tao, Electron transport in single molecules: from benzene to graphene, Acc. Chem. Res. 42 (2009) 429–438.
[7] K.S. Novoselov, A.K. Geim, S.V. Morozov, D. Jiang, Y. Zhang, S.V. Dubonos, I.V. Grigorieva, A.A. Firsov, Electric field effect in atomically thin carbon films, Science 306 (2004) 666–669.
[8] D.A. Areshkin, D. Gunlycke, C.T. White, Ballistic transport in graphene nanostrips in the presence of disorder: importance of edge effects, Nano Lett. 7 (2007) 204–210.
[9] K. Nakada, M. Fujita, G. Dresselhaus, M.S. Dresselhaus, Edge state in graphene ribbons: nanometer size effect and edge shape dependence, Phys. Rev. B 54 (1996) 17954–17961.
[10] Y.W. Son, M.L. Cohen, S.G. Louie, Energy gaps in graphene nanoribbons, Phys. Rev. Lett. 97 (2006) 216803.
[11] M.Y. Han, B. Oezyilmaz, Y. Zhang, P. Kim, Energy band-gap engineering of graphene nanoribbons, Phys. Rev. Lett. 98 (2007), 206805.
[12] R.R. Nair, P. Blake, A.N. Grigorenko, K.S. Novoselov, T.J. Booth, T. Stauber, A.K. Geim, Fine structure constant defines visual transparency of graphene, Science 320 (2008) 1308.
[13] A. Yu, P. Ramesh, M.E. Itkis, E. Bekyarova, R.C. Haddon, Graphite anoplateletepoxy composite thermal interface materials, J. Phys. Chem. C 111 (2007) 7565–7569.
[14] J. Park, Y.H. Ahn, C. Ruiz-Vargas, Imaging of photocurrent generation and collection in single-layer graphene, Nano Lett. 9 (2009) 1742.
[15] E.J.H. Lee, K. Balasubramanian, R.T. Weitz, M. Burghard, K. Kern, Contact and edge effects in graphene devices, Nat. Nanotechnol. 3 (2008) 486–490.
[16] F. Xia, T. Mueller, R. Golizadeh-Mojarad, M. Freitag, Y. Lin, J. Tsang, V. Perebeinos, P. Avouris, Photocurrent imaging and efficient photon detection in a graphene transistor, Nano Lett. 9 (2009) 1039.
[17] F. Xia, T. Mueller, Y.M. Lin, A.P. Valdes-Garcia, Avouris, ultrafast graphene photodetector, Nat. Nanotechnol. 4 (2009) 839–843.
[18] T. Mueller, F. Xia, P. Avouris, Graphene photodetectors for high-speed optical communications, Nat. Photonics 4 (2010) 297–301.
[19] M. Lemme, F.H.L. Koppens, A.L. Falk, M.S. Rudner, H. Park, L.S. Levitov, C.M. Marcus, Gate-activated photoresponse in a graphene p–n junction, Nano Lett. 11 (2011) 4134–4137.
[20] J.C.W. Gabor, Q. Song, N.L. Ma, T. Nair, K. Taychatanapat, T. Watanabe, L.S. Taniguchi, Hot carrier—assisted intrinsic photoresponse in graphene, Science 334 (6056) (2015) 648–652.
[21] J.C.W. Song, M.S. Rudner, C.M. Marcus, L.S. Levitov, Hot carrier transport and photocurrent response in graphene, Nano Lett. 11 (2011) 4688–4692.
[22] F.H.L. Koppens, D.E. Chang, F.J. García de Abajo, Graphene plasmonics: a platform for strong light–matter interactions, Nano Lett. 11 (2011) 3370–3377.
[23] X. Zhou, X. Huang, X. Qi, S. Wu, C. Xue, Q. Yan, P. Chen, H. Zhang, In situ synthesis of metal nanoparticles on single-layer graphene oxide and reduced graphene oxide surfaces, J. Phys. Chem. 113 (10) (2009) 842–10846.
[24] A.P. Alivisatos, Semiconductor clusters, nanocrystals, and quantum dots, Science 271 (1996) 933–937.
[25] A.K. Geim, Graphene: Sstatus and prospects, Science 324 (2009) 1530–1534.
[26] A. Cao, Z. Liu, S. Chu, M. Wu, Z. Ye, Z. Cai, Y. Chang, S. Wang, Q. Gong, Y. Liu, A Facile One-step method to produce graphene–CdS quantum dot nanocomposites as promising optoelectronic materials, Adv. Mater. 22 (2010) 103–106.
[27] G. Konstantatos, M. Badioli, L. Gaudreau, J. Osmond, M. Bernechea, F.P. Garcia de Arquer, F. Gatti, F.H.L. Koppens, Hybrid graphene-quantum dot phototransistors with ultrahigh gain, Nat. Nanotechnol. 7 (2012) 363–368.
[28] K.S. Novoselov, A.H.C. Neto, Two-dimensional crystals-based heterostructures: materials with tailored properties, Phys. Scr. T146 (2012) 014006.
[29] A.H.C. Neto, K.S. Novoselov, New directions in science and technology: two dimensional crystals, Rep. Prog. Phys. 74 (2011) 082501.
[30] B. Radisavljevic, A. Radenovic, J. Brivio, V. Giacometti, A. Kis, Single-layer MoS_2 transistors, Nat. Nanotechnol. 6 (2011) 147–150.
[31] S. Kim, A. Konar, W.S. Hwang, J.H. Lee, J. Lee, J. Yang, C. Jung, H. Kim, J.B. Yoo, J.Y. Choi, High-mobility and low-power thin-film transistors based on multilayer MoS_2 crystals, Nat. Commun. 3 (2012) 1011.
[32] J. Pu, Y. Yomogida, K.K. Liu, L.J. Li, Y. Iwasa, T. Takenobu, Highly flexible MoS_2 thin-film transistors with ion gel dielectrics, Nano Lett. 12 (2012) 4013–4017.
[33] J. Yoon, W. Park, G.Y. Bae, Y. Kim, H.S. Jang, Y. Hyun, S.K. Lim, Y.H. Kahng, W.K. Hong, B.H. Lee, Highly flexible and transparent multilayer MoS_2 transistors with graphene electrodes, Small 9 (2013) 3295–3300.
[34] L. Tianshu, G. Giulia, Electronic properties of MoS_2 nanoparticles, J. Phys. Chem. C 111 (2007) 16192–16196.
[35] S. Das, H.Y. Chen, A.V. Penumatcha, J. Appenzeller, High performance multilayer MoS_2 transistors with scandium contacts, Nano Lett. 13 (2013) 100–105.
[36] S. Bertolazzi, J. Brivio, A. Kis, Stretching and breaking of ultrathin MoS_2, ACS Nano 5 (2011) 9703–9709.
[37] Y.L. Huang, Y. Chen, W. Zhang, S.Y. Quek, C.H. Chen, L. Li, W.T. Hsu, W.H. Chang, Y.J. Zheng, W. Chen, A.T.S. Wee, Bandgap tunability at single-layer molybdenum disulphide grain boundaries, Nat. Commun. 6 (2015) 6298.
[38] Z. Yin, H. Li, H. Li, L. Jiang, Y. Shi, Y. Sun, G. Lu, Q. Zhang, X. Chen, H. Zhang, Single-layer MoS_2 phototransistors, ACS Nano 6 (2012) 74–80.
[39] D.S. Tsai, K.K. Liu, D.H. Lien, M.L. Tsai, C.F. Kang, C.A. Lin, L. Li, J. He, Few-layer MoS_2 with high broadband photo gain and fast optical switching for use in harsh environments, ACS Nano 7 (2013) 3905–3911.
[40] W.J. Zhang, J.K. Huang, C.H. Chen, Y.H. Chang, Y.J. Cheng, L.J. Li, High gain phototransistors based on a CVD MoS_2 monolayer, Adv. Mater. 25 (2013) 3456–3461.
[41] O. Lopez-Sanchez, D. Lembke, M.A. Radenovic, A. Kis, Ultrasensitive photodetectors based on monolayer MoS_2, Nat. Nanotechnol. 8 (2013) 497–501.
[42] K. Chang, W.X. Chen, In situ synthesis of MoS_2/graphene nanosheet composites with extraordinarily high electrochemical performance for lithium ion batteries, Chem. Commun. 74 (14) (2011) 4252–4254.
[43] Y.M. Shi, W. Zhou, A.Y. Lu, W.J. Fang, Y.H. Lee, A.L. Hsu, Van der Waals epitaxy of MoS_2 layers using graphene as growth templates, Nano Lett. 12 (2012) 2784–2791.
[44] K. Chang, W.X. Chen, L-Cysteine-assisted synthesis of layered MoS_2/graphene composites with excellent electrochemical performances for lithium ion batteries, ACS Nano 5 (2011) 4720.
[45] D.V. Kosynkin, A.L. Higginbotham, A. Sinitskii, J.R. Lomeda, A. Dimiev, B.K. Price, J.M. Tour, Longitudinal unzipping of carbon nanotubes to form graphene nanoribbons, Nature 458 (2009) 872–876.
[46] M. Asad, M. Fathipour, M.H. Sheikhi, M. Pourfath, High-performance infrared photo-transistor based on SWCNT decorated with PbS nanoparticles, Sens. Actuators A 220 (2014) 213–220.
[47] M. Asad, M.H. Sheikhi, M. Pourfath, M. Moradi, High sensitive and selective flexible H2S gas sensors based on Cu nanoparticle decorated SWCNTs, Sens. Actuators B 210 (2015) 1–8.
[48] Z. Lu, C.X. Gou, H.B. Yang, Y. Qiao, J. Guo, C.M. Li, One-step aqueous synthesis of graphene-CdTe quantum dot-composed nanosheet and its enhanced photoresponse, J. Colloid Interface Sci. 353 (2011) 588–592.
[49] S. Stankovich, D.A. Dikin, R.D. Piner, K.A. Kohlhaas, A. Kleinhammes, Y. Jia, Y. Wu, S.T. Nguyen, R.S. Ruoff, Synthesis of graphene-based nanosheets via chemical reduction of exfoliated graphite oxide, Carbon 45 (2007) 1558–1565.
[50] A. Sinitskii, A. Dimiev, D.V. Kosynkin, J.M. Tour, Graphene nanoribbon devices produced by oxidative unzipping of carbon nanotubes, ACS Nano 4 (9) (2010) 5405–5413.
[51] G.L. Frey, R. Tenne, M.J. Matthews, M.S. Dresselhaus, G. Dresselhaus, Raman and resonance Raman investigation of MoS_2 nanoparticles, Phys. Rev. B 60 (1999) 2883–2892.
[52] M. Cardona, Light Scattering in Solids II, in: M. Cardona, G. Guntherödt (Eds.), Springer-Verlag, Berlin, 1983, p. 19.
[53] R.J. Nemanich, S.A. Solin, First- and second-order Raman scattering from finite-size crystals of graphite, Phys. Rev. B 20 (1979) 392–401.
[54] J.L. Zhang, H.J. Yang, G.X. Shen, P. Cheng, J.Y. Zhang, S.W. Gou, Reduction of graphene oxide via L-ascorbic acid, Chem. Commun. 46 (2010) 1112–1114.
[55] Y. Zhou, Q.L. Bao, L.A.L. Tang, Y.L. Zhong, K.P. Loh, Hydrothermal dehydration for the green reduction of exfoliated graphene oxide to graphene and demonstration of tunable optical limiting properties, Chem. Mater. 21 (2009) 2950–2956.
[56] D. Li, M.B. Muller, S. Gilje, R.B. Kaner, G.G. Wallace, Processable aqueous dispersions of graphene nanosheets, Nat. Nanotechnol. 3 (2008) 101–105.
[57] T.P. Prasad, E. Diemann, A. Moller, Thermal decomposition of $(NH_4)_2MoO_2S_2$, $(NH4)_2MoS_4$, $(NH_4)_2WO_2S_2$ and $(NH_4)_2WS_4$, J. Inorg. Nucl. Chem. 35 (1973) 1895–1904.
[58] W. Zhang, C. Chuu, J. Huang, C. Chen, M. Tsai, Y. Chang, C. Liang, Y. Chen, Y. Chueh, J. He, M. Chou, L. Li, Ultrahaigh-gain phototransistors based on atomically thin graphene-MoS_2 heterostructures, Sci. Rep 4 (2014) 3826.
[59] X. Li, J. Wu, N. Mao, J. Zhang, Z. Lei, Z. Liu, H. Xu, A self-powered graphene–MoS_2 hybrid phototransistor with fast response rate and high on-off ratio, Carbon 92 (2015) 126–132.
[60] F. Wang, Y. Zhang, C. Tian, C. Girit, A. Zettl, M. Crommie, Y.R. Shen, Gate-variable optical transitions in graphene, Science 320 (2008) 206–209.
[61] T. Koppens, A.C. Avouris, M.S. Ferrari, M. Polini, Photodetectors based on graphene, other two-dimensional materials and hybrid systems, Nat. Nanotechnol. 9 (2014) 780–793.

Biographies

Mohsen Asad is a research engineer at the Semiconductor Device Research Center, School of Electrical and Computer Engineering, Shiraz University, Iran. He has been worked about three years at MEMS & NEMS Lab under supervisory of Prof. Fathipour at University of Tehran, Iran. His research interests include developing process and fabricating prototype flexible electronics and optoelectronic devices based on semiconductor science and physics of quantum materials.

Sedigeh Salimian is a PhD student on Solid state physics at Kharazmi University, Tehran, Iran. Her research interests include characterization and processing of semiconductor quantum dots, organic nanocomposites, graphene nanoribbons and novel nanomaterials like MoS2 for development in applications such as transistors and sensors.

Mohammad Hossein Sheikhi received his BSc (1994) degree in electrical engineering from Shiraz University, Shiraz, Iran, the MSc (1996) degree from Sharif University of Technology, Tehran, Iran and the PhD degree in electrical engineering from TarbiatModarres University, Tehran in 2000. Dr. Sheikhi was selected as the distinguished PhD student graduated from TarbiatModarres University in 2000. He joined Tohokou University, Sendai, Japan, as a Research Scientist in 2000. After joining Shiraz University in 2001, he focused on the optoelectronics, nanosensors, and nanotransistors. He is currently the Associate Professor and founder of Semiconductor Device Research Center, Shiraz University, Shiraz, Iran.

Mahdi Pourfath was born in Tehran, Iran, in 1978. He received the B.S and M.S. degrees in electrical engineering from Sharif University of Technology, Tehran, in 2000 and 2002, respectively, and the Ph.D. degree in Microelectronics from the TechnischeUniversität Wien, Austria, in 2007. He has authored or co-authored over 100 scientific publications and presentations and authored one monograph. He is now an Assistant Professor in the School of Electrical and Computer Engineering, University of Tehran. He is also with the institute of Microelectronics, TechnischeUniversität Wien, Austria. His scientific interests include novel nanoelectronic devices and materials.